Design and analysis of 2D photonic crystal wavelength routers using micro-ridge and arc waveguides

HARKIRANJEET KAUR*, R. S. KALER, BALVEER PAINAM
Thapar University, ECE Department, Optical Fiber Communication Research Laboratory (OFCR Lab), Patiala, Punjab, India, 147004

In this paper, (1x2) T-shaped wavelength router is devised on two dimensional square photonic crystals lattice. The conventional tapered ridge waveguides and arc waveguide of comparatively low dielectric constant are introduced in the crystal structure. These waveguides facilitate the light transmission from the input port to output ports. The transmission spectrum for this structure is analysed using Finite-Difference Time-Domain (FDTD) approach. The results indicate that the designed router can separate the wavelengths of 1.52 µm and 1.6 µm with the power efficiency as high as 99.9%. The minimum crosstalk obtained for the router is -29.48 dB.

(Received July 7, 2015; accepted September 29, 2016)

Keywords: Photonic Crystal (PhC), Crosstalk, Band-gap, Conventional ridge waveguide, Plane Wave Expansion (PWE) method

1. Introduction

In the recent few decades, photonic crystals [1, 2] have provided the potential platform for wide range of applications in numerous domains. Many optical communication devices such as multiplexers/de-multiplexers [3], interleavers [4], filters [5] etc., designed on the photonic crystals have been reported showing high throughputs. Since the photonic crystal devices have made a significant contribution in the areas of compactness, miniature sizes and fast switching etc., many wavelength routers are also designed using photonic crystals [6-9].

Wavelength routers are one of the building blocks of optical switch circuits. The routersroute the signal launched at the input port to different output ports based on the wavelengths constituting the signal. This routing mechanism is obliged by the resonant wavelengths of various routing elements present along the transmission path of the signal. Therefore, the input signal is de-multiplexed into different resonant wavelengths and these wavelengths are optically switched to their respective output ports. Photonic crystal routers consist of straight waveguides, formed by removing a series of crystal rods. The resonating cavities are introduced in the routers to improve their selectivity [6]. Crosstalk is an important parameter for the analysis of performance of routers as it is the degree of interference of two signals. The crosstalk between two ports can be calculated as the difference in the transmittances in decibels, i.e. $CT_{i,j}= T_j-T_i$, where CT_{ij} is the crosstalk between port 'i' and port 'j' and T_i, T_j are the transmittances of ports 'i' and 'j' respectively[7].

Giovanna Calo et al. [7] devised the (1x2) basic cross wavelength routers based on photonic crystal ring resonators. A number of such routers are assembled into a single structure to form higher order router matrices. Authors have designed the resonant ring structures, which can be tuned by varying the radius of central rods of ring to optimize the performance of routers.Wei Yu Chiu et al. [8] demonstrated the silicon on insulator 2D ring resonators based on hexagonal photonic crystal lattice. These ring resonators act as routers, routing the two wavelengths of 1.31µm and 1.55 µm to their respective output ports. The nano structures of this device are fabricated using E-beam lithography technique. Authors have optimized the radius of nano-rods to reduce optical loss and crosstalk problem. T. N. Bakhvalova et al.[9] proposed and investigated the 2D photonic de-multiplexer which outputs different wavelengths used in telecommunication. Authors have introduced various nano filters such as defective rods, tapered waveguides etc. within the photonic crystal T-junction waveguide to have selective radiation of light.These nano-devices modify the behaviour of a structure to a large extent.

In the above literature, various routers are analysed for their performance as a switching device. The (1x2) broadband router discussed [7] is scalable and is also used in (4x4) configuration using eight such routers. The minimum crosstalk obtained for this router is approximately -16dB within the range of 1.48 µm -1.55 µm. The ring resonator device illustrated in [8] has conventional silicon ridge waveguides at the input and output ports for ensuring the lossless transition of light into and from the photonic crystal waveguide. The advantage of the de-multiplexer demonstrated in [9] is its miniature size. However, this device has low drop efficiency and low insulation.

Previously, we have reported PCW biochemical sensor for the estimation of chemical concentration [10], active layer identification of PCW biosensor chip for the detection of *Escherichia coli* [11] and all optical NOR gate based on cross structures in 2D photonic crystal using logic NOT and OR gate [12]. In this paper, we have

designed the wavelength router based on 2D square photonic crystal lattice having Si rods embedded in air wafer. The conventional photonic waveguides of relatively lower refractive index (SiO_2) are introduced at various points in the photonic crystal waveguides (air). These waveguides break the periodicity of photonic crystal and direct the input signal towards the output ports with extremely low losses. It is due to the total internal reflection phenomenon suffered by light rays in these guides. The transmission spectrum of router is analyzed using FDTD approach. The crosstalk between two outputs is also calculated as it indicates the degree of interference between the different signals.

This paper is organized as follows. In section 2, the simulation set up of the photonic crystal wavelength routers is described. It discusses all line defects and various conventional waveguides introduced in photonic crystal layout to form router. In section 3, the results of PWE and FDTD simulations are discussed. Section 4 concludes the paper.

2. Simulation set up

The wavelength router is designed on the square photonic crystal lattice (in X-Z plane) having Si rods of refractive index 3.47 placed in an air wafer. The substrate is made up of quartz (Silica) having refractive index of 1.45. A T-shaped wavelength router is formed by removing the silicon rods from the crystal in a straight line, thus introducing the line defects. One complete horizontal straight waveguide and the other quasi vertical waveguide intersect to form the T-shape as shown in Fig. 1(a). Also, the conventional photonic waveguides of refractive index same as substrate (quartz) are introduced in the router, i.e. two tapered ridge waveguides are placed towards the output ports and an arc shaped waveguide is placed exactly at the middle of the T-junction. Both of these waveguides have height of only 1µm in the vertical Y-direction. The radius of silicon rods in the crystal is 0.32 times the lattice constant 'a', where the lattice constant for this router is 0.682 µm.

FDTD method is used to simulate the structure; in this environment radiation losses in the vertical direction are neglected. In practical fabricated device, the similar performance of theoretical ones should require the realization of omnidirectional reflectors on and below the 2D PhC structures to guarantee efficient light confinement in the vertical direction [13]. The diameter (d) of the cylindrical silicon rod in air is 0.436 µm, lattice constant (a) is 0.682 µm and normalized hole size (r/a) is 0.32. These are the well suited parametric dimensions for the fabrication of micro rigid and arc waveguide 2D photonic crystal wavelength router device on silica.

Above the tapered ridge waveguides, are placed the defective silicon rods marked in red color in Fig. 1(a), having half the radius of the crystal rods. The ports marked as 'right' and 'bottom' are the output ports and input signal is launched through the port marked as 'input'. To the extreme left of the structure in Fig. 1(a) is the red colored vertical input plane. The input signal is launched in the +z direction through this plane. In the Fig. 1(b) and 1(c), the top and side view of designed router is shown, in terms of the variation of refractive index in the vertical Y-direction. Silicon rods of higher refractive index are appearing in the red color at the top, whereas the substrate and the conventional waveguides are in the blue color, which are of lower refractive indices of 1.45.

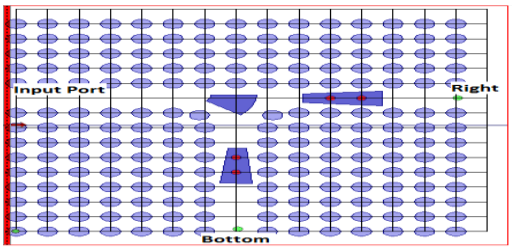

(a)

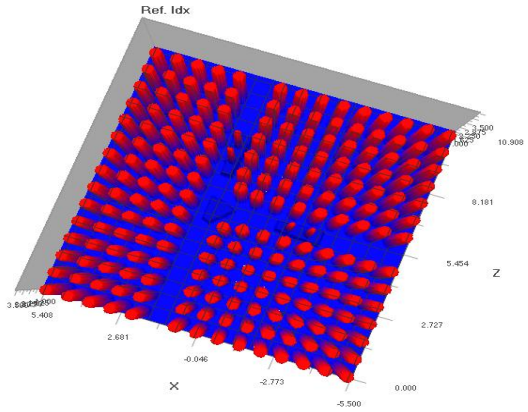

(b)

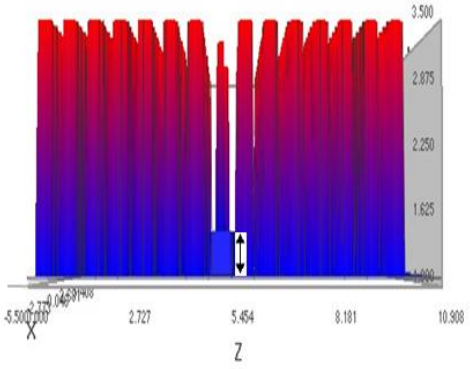

(c)

Fig. 1. (a) Simulation setup of the wavelength router. (b) 3D Topview of the router structure. (c) 3D side view of the router (ridge waveguide of 1µm is marked with a black arrowed line having silicon rods above it)

The significance of conventional waveguides in this structure is their ability to guide light through the mechanism of total internal reflection. Where photonic crystals provide efficient confinement for the light signal owing to their band-gap, the conventional waveguides are placed in the air as light easily scatters in the low index

material. These are the quartz base below the defective rods inside the photonic waveguides, which not only provides the vertical confinement but also reduces the scattering losses. The tapering of ridge waveguides is done towards the intersection. The defective silicon rods above the ridges are responsible for good selectivity of the router. The arc waveguide at the intersection is mainly for smooth transition of input signal towards the output ports. The variation of output signal with change in arc radius is also studied in this work.

3. Results and discussions

Photonic band-gap for the designed wavelength router is calculated using Plane-Wave Expansion method (PWE) [14]. The TE modes band gaps for the defect-free router configuration lie between the ranges 1/λ (1/μm) equals to 0.57438 - 0.712168 and 0.3299- 0.413818. We consider the first band gap having higher frequencies i.e. 0.57438 - 0.712168 (1/μm) which represents the range of wavelengths of our interest i.e.1.404 to 1.741 μm. However, no band gaps are observed in TM modes. The k-vector scale of graphs in Fig. 2 is indexed 0-15 in the first Brillouin zone [2], representing the range [0-2π/a], and 'a' is the lattice constant (where any index 'i' corresponds to wave vector (2π/ (15a)* 'i') in reciprocal lattice). This region is a set of non- equivalent wave vectors closest to the wave vector k=0.

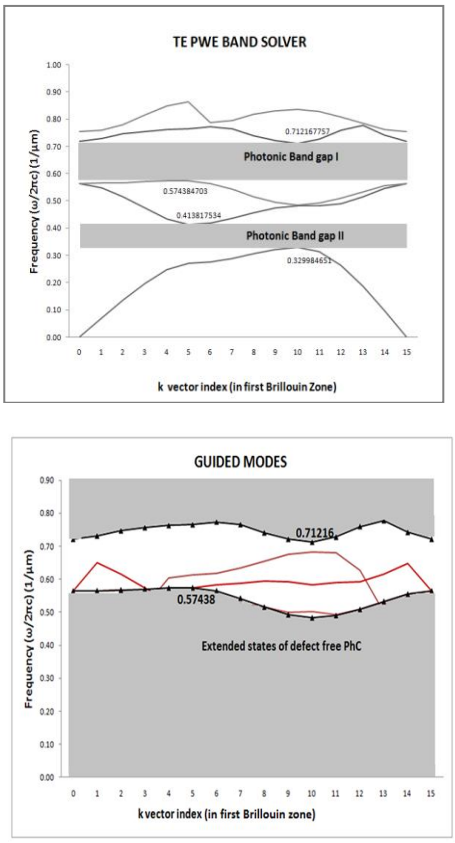

Fig. 2. (a) TE Photonic band gap of defect free photonic crystal router. (b) Guided TE modes of wavelength router with defects (shown as red lines) within the first band gap

We observe that every dispersion curve in the Fig. 2 has same value of frequencies at the k-vector index equals to 0 and at index equals to 15. This is due to the fact that this region represents non redundant wave vectors following the rotational symmetry. Beyond this region, same band gap structure repeats itself. Therefore, the ends overlap the dispersion curves at the values the curves started.

With the introduction of line defects in the photonic crystal to carve a T-shaped junction router, the photonic band gap disappears with the inception of guided modes inside it. The propagation of these light modes is possible within the waveguides formed by defects. In Fig. 2(b), guided transverse electric modes are shown in red color. The grey shaded region is representing the extended states of defect free crystal, i.e. this region has no change in the band structure even after defects are formed, except the band gaps no longer exist.

The power transmission curves are calculated using Finite-Difference Time-Domain approach [15]. The input is 'Gaussian' wave launched through the vertical plane. The efficiency of designed wavelength router is optimized by changing the radius of an arc in the middle of T-junction. The variation of maximum power output efficiency for both the output ports with an arc radius is studied as shown in Fig. 3. The results show that maximum power efficiency is attained for the radius of 0.892 μm, where right port has 99.9 % and bottom output port has 99.5% output efficiency at their respective resonant wavelengths. Therefore, the complete transmission spectrum for the router is analyzed at the radius of 0.892 μm as discussed below.

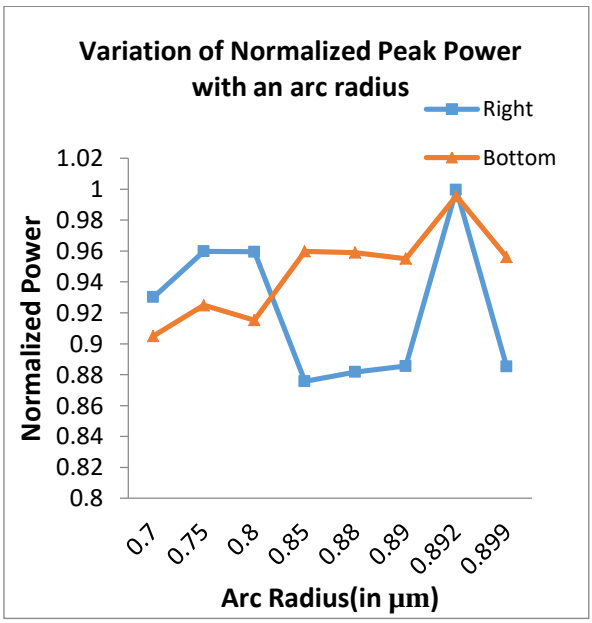

Fig. 3. Variation of peak normalized power with change in an arc radius

The transmission spectrum of wavelength router is shown in Fig. 4. In Fig. 4(a), the power spectrum is

plotted, which is normalized with respect to the input plane. The results show the maximum throughputs of 0.999 and 0.995 are attained at the wavelengths 1.52 µm and 1.6 µm for right and bottom port respectively. The value of crosstalk is also calculated between the output ports at these two operating wavelengths of the router from the Fig. 4(b).

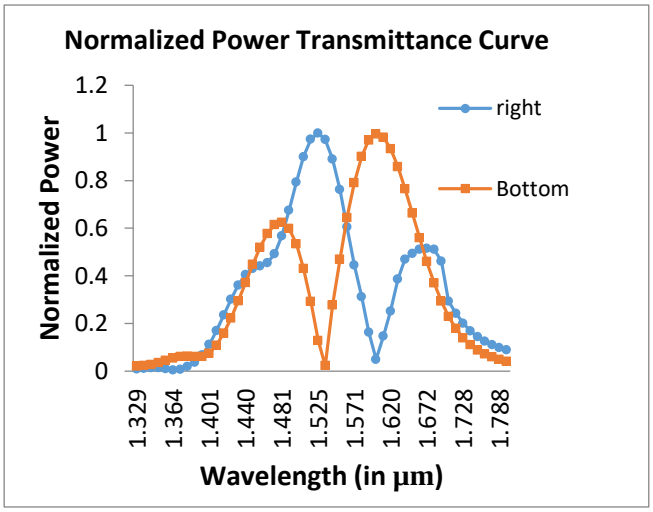

(a)

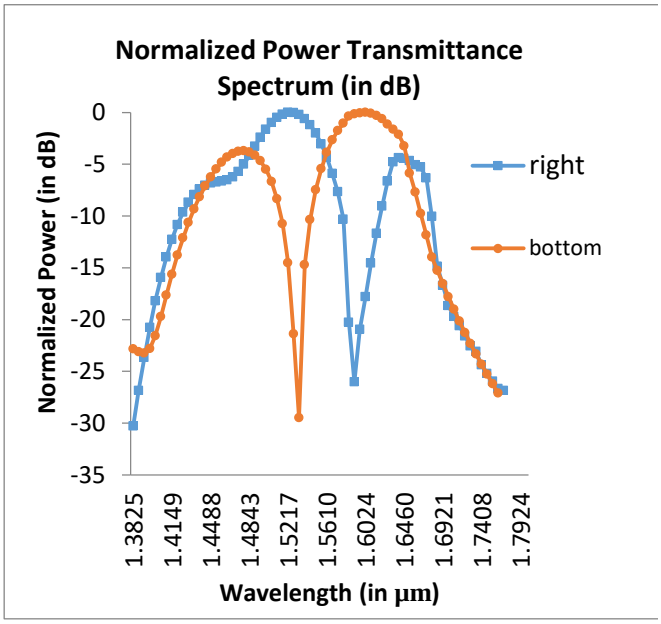

(b)

Fig. 4. (a) Normalized power transmittance curve of router with an arc radius of 0.892 µm. (b) Power transmittance curve of router in decibels

From the Fig. 4(b), to calculate crosstalk between two output ports, we have transmittances as -0.0125 dB and -29.5 dB at 1.52 µm and -0.0151 dB and -26.99 dB at 1.6 µm for the output ports present at the right and the bottom of router respectively. Crosstalk is the difference between both the outputs in decibels. For right output port at 1.52 µm, it is calculated as T_{bottom}-T_{right}, which is equal to -29.48 dB. Similarly for bottom output port at the wavelength of 1.6 µm, it is equal to -26.974 dB. The calculated crosstalk for both the cases is sufficiently low for an efficient performance of a router.

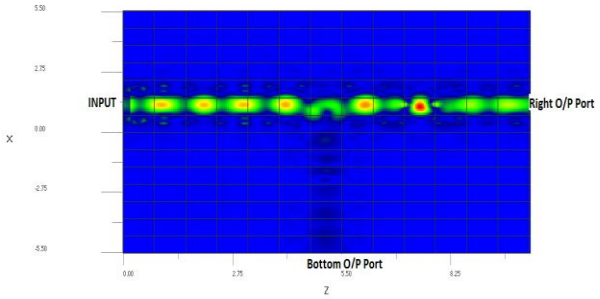

(a)

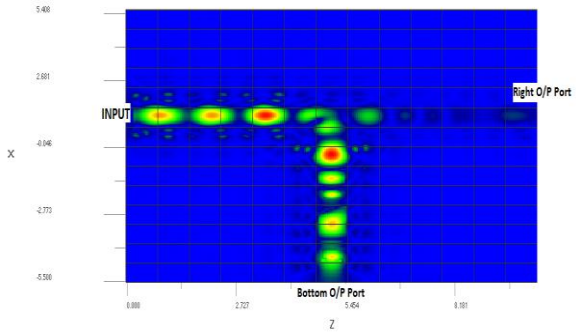

(b)

Fig. 5. (a) Electric field distribution Image Map for wavelength router at input wavelength of 1.52 µm. (b) E-field Image Map at input wavelength of 1.6 µm

The electric field image maps given in Fig. 5 are the clear depiction of results calculated above. In Fig. 5(a), the complete transfer of input signal power is towards the right output port of the router, simulated at the wavelength of 1.52 µm. And in Fig. 5(b), the input power is transferred to the bottom port of the router, which is analyzed at the wavelength of 1.6 µm, showing negligible transfer to the other port.

4. Conclusion

The wavelength router configuration designed in this paper is analyzed using FDTD approach. The conventional tapered ridge waveguides and an arc waveguide of Silica are introduced in the T-junction of photonic crystal waveguides formed. These waveguides facilitate the lossless transmission of input light towards the output ports. The designed structure splits the wavelengths of 1.52 µm and 1.6 µm to the right and bottom output ports of router respectively with output efficiency of 99% in both the cases. The minimum crosstalk calculated for this device is -29.48 dB. Therefore, this device is suitable for

low loss integrated circuits with minimal interference among different outputs.

References

[1] E. Yablonovitch, Physical Review Letters **58,** 2059 (1987).

[2] J. D. Joannopoulos, R. D. Meade, J. N. Winn, Princeton University Press, Princeton, (2008).

[3] B. Kumar, V. Suthar, K. S. Kumar, A. Singh, Progr. Electromag. Res. Lett. **33**, 27 (2012).

[4] Yu-Jun Quan, P. D. Han, Xiao-Dong Lu, Zhi-Cheng Ye, Li Wu, Optics Communications **27**, 203 (2007).

[5] C. J. Wu, M. H. Lee, W. H. Chen, T. J. Yang, J. Electromagnatic Waves Appl. **25**, 1360 (2011).

[6] Solomon Assefa, Peter T. Rakich, Peter Bienstman, Steven G. Johnson, Gale S. Petrich, John D. Joannopoulos, Leslie A. Kolodziejski, Erich P. Ippen, Henry I. Smith, Applied Physics Letters **85**, 6110 (2004).

[7] Giovanna Calo, Vincenzo Petruzzelli, IEEE Journal of Photonics **5**, 1011 (2013).

[8] Wei-Yu Chiu, Tai-Wei Huang, Yen-Hsiang Wu, Yi-Jen Chan, Chia-Hung Hou, Hung-Ta Chien, Chii-Chang Chen, Optical Express **15**, 155 (2007).

[9] T. N. Bakhvalova, I. V. Khmelnitsky, Progress In Electromagnetics Research Symposium Proceedings, Moscow, Russia, 2012, pp. 1143.

[10] B. Painam, P. Teotia, R. S. Kaler, M. Kumar, 12th International Conference on Fiber Optics and Photonics, OSA Technical Digest (online) (Optical Society of America, 2014), paper S5A.48.

[11] B. Painam, R. S. Kaler, M. Kumar, Optical Engineering **55**(7), 077105 (2016).

[12] D. Rani, R. S. Kaler, B. Painam, Journal of Optical Technology (In press).

[13] G. Calò, V. Petruzzelli, IEEE Photonics Journal **5**(3), 7901011 (2013).

[14] J. B. Pendry, Journal of Physics: Condensed Matter **8**, 1085 (1996).

[15] A. Taflove, Artech House, Boston, London (2005).

*Corresponding author: harkiranjeet19@gmail.com